

BENDING BEHAVIOR OF CFRP-REINFORCED THINWALLED METAL BEAMS – A THEORETICAL AND EXPERIMENTAL STUDY

M. Oxenbauer¹ and K. Rother²

¹BMW AG and University of Applied Sciences Munich, Knorrstraße 147, D-80788 München,
Germany, Email: marco.oxenbauer@bmw.de

²Department of Mechanical, Automotive and Aeronautical Engineering, University of Applied
Sciences Munich, Lothstr. 64, 80335 München, Germany, Email: klemens.rother@hm.edu

Keywords: CFRP-metal-hybrid, experimental, bending, numerical, analytical

Abstract

Structural CFRP reinforced metal parts can open new opportunities in car body design and many other industrial applications. Selection of a the right material and dimensions at the right spot requires improved methods in for development. The targeted manipulation of required properties and higher material utilization implied a high potential of lightweight design. The tested CFRP reinforced square hollow section aluminum and steel profiles offered different possibilities to influence the part performance and shows the effect of the rate of reinforcement and design. A theoretical consideration of the experiments shows further capabilities for lightweight design.

1. Introduction

Due to strict legal regulations the automotive industry has to face challenges to reduce CO₂ emmissions and fulfill safety requirements. To achieve the environmental aspect one approach is to reduce the weight of the vehicle. This can be succeeded by introducing new materials like carbon fiber reinforced plastics (CFRP) to a high volume production, better utilization of material limits and new approaches in material designing concepts of components, like combining two or more within one part. With the mixture of two materials, new mechanical properties can be generated, a monolithic structural element can not achieve. Also cost efficiency aspects could better be achieved by hybrid technologies. To gain expertise of the behavior of these constructions, various investigations has been carried out. For example Bambach, et. al. [1][2] dealed with glass and carbon fiber reinforced metal tubes under axial loading cases, while Kim [3] deals with a FEA modeling of collapsing CFRP strengthened bending beams and Jung [4] handle glass fiber cracking in hybrid beams under transversal loading. The next nessessary further step is the implementation previous studies in the designing process of car body parts and close further gaps in knowledge. Because of the enlarged number of free parameters to choose during structural design, hybrid components are significant more complex than monolithics. A possible procedure to find an optimum draft of a part is described in [5], by a modular, analytical analysis method which allows a parametrical optimization of hybrid structures. The objective of the current work is to confirm and compare these theoretical calculations with experimental data and give a qualitative discription of the effectiveness of different CFRP reinforced steel and aluminum bending beams.

2. Specimen and experimental setup

In view of an automotive application, two interesting types of metal materials were investigated. The cross section of the AW6060 aluminum extrusion has an outer dimension of 60x60mm and a overall wallthickness of 2,0mm (square hollow section SHS). For the dualphasesteel CR440Y780-DP specimen, two cap profiles with a wall thickness of 0.7mm were joined by spotwelding (dubble cap profile DHP) to form a hollow bar (Figure 1). Both types of specimen have a length of 1000mm.. A unidirectional CFRP layup with PREPREG PR-UD CS 300/600 FT102 38 were used to reinforce the flanges of the metal profiles, while a symmetrical and balanced $\pm 45^\circ$ layup were used for web reinforcement. The CFRP is bonded to the aluminum bar by 2k epoxid base TEROSON EP 5065 (Henkel). Steel CFRP connection is realized with Betamate 2098 (Dow Automotive). The basis properties of the tested materials are shown in Table 1 and the specimen details in Table 2.

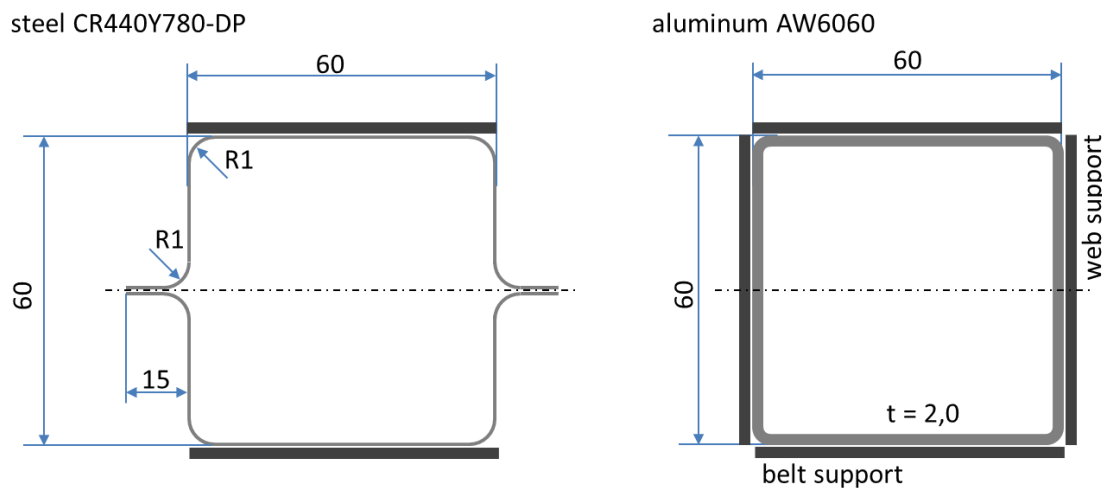


Figure 1. Steel DHP and aluminum SHS specimen

The aluminum und steel members were tested under a four point bending load by a Schenk/Trebel 100kN universal testing maschine with an accuracy class 0.5. The testing maschine was instrumented with an internal quartz crystal load cell and the displacement was measured with an external high-resolution inductive displacement transducer. Both were logged with 10 Hz. Additionally a high-definition digital video was recorded during the tests with 30 frames/seconds. The outer support span of the test setup was $L = 900mm$, the hinged inner supporting span was $l = 200mm$, while the roll diameter of the supports were $R = 60mm$. The quasistatic testing speed of the SHS and DHP were $5 mm/min$ by a maximum possible vertical displacement of $s = 85 mm$. The specimen and loading condition is representing a typical loading case within the automotive car body. The CFRP reinforcement shows the potential of hybrid design.

Table 1. Material data

Material	E_1 (GPa)	E_2 (GPa)	R_p (MPa)	R_m or X_t (MPa)	ρ (g/cm ³)
CR440Y780-DP	210	210	470	780	7.8
AW6060	70	70	140	240	2.7
PR-UD CS 300/600	126	9		2300	1.54

Table 2. CFRP reinforcements for the different specimens

specimen	metal	upper flange 0°-UD (mm)	lower flange 0°-UD (mm)	web ±45° (mm)
SHS1	AW6060 (2mm)	-	-	-
SHS2	AW6060 (2mm)	2	-	-
SHS3	AW6060 (2mm)	-	2	-
SHS4	AW6060 (2mm)	2	2	-
SHS5	AW6060 (2mm)	-	-	2
SHS6	AW6060 (2mm)	2	2	2
SHS7	AW6060 (2mm)	4	4	-
DHP1	CR440Y780-DP (0.7mm)	-	-	-
DHP2	CR440Y780-DP (0.7mm)	2	-	-
DHP3	CR440Y780-DP (0.7mm)	-	2	-
DHP4	CR440Y780-DP (0.7mm)	4	-	-
DHP5	CR440Y780-DP (0.7mm)	-	4	-
DHP6	CR440Y780-DP (0.7mm)	2	2	-

3. Three point bending test results

Below the qualitative failing behavior and the quantitative properties of the tested specimen are described. This aims on a better understanding in which way thinwalled hybrid bending beams behave in case of a bending load like it can appears in a car body.

3.1. Qualitative behavior of hybrid bending beams - failure mode

The specimen failed due to the different reinforcement design in different failure modes. The all aluminum sample SHS1 failed due to a local plastic flange buckling at the location of the force application. The unidirectional CFRP reinforcement of SHS2 stabilizes the aluminum profile after reaching its yield strength, so there was no buckling of the compression flange at the top. The unreinforced bottom flange loaded in tension plasticizes and bended inwards, while there is a smooth flatten of the force level. The CFRP failed abrupt by a mixture of compressive stress and local bending at a high displacement of the beam.

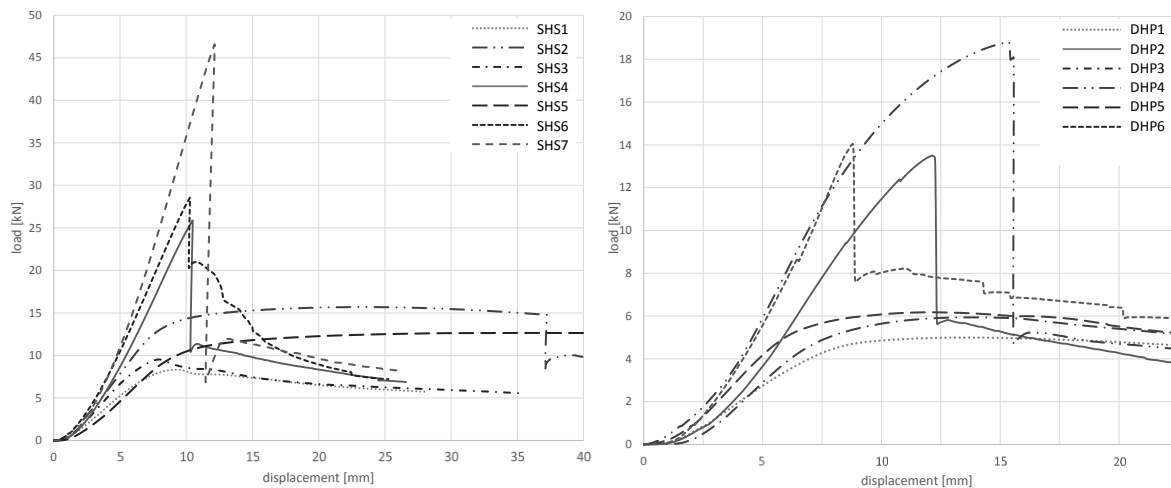


Figure 2. Experimental force-displacement curves of aluminum and steel variants.

Excerpt from ISBN 978-3-00-053387-7

The SHS3 specimen showed beside a higher bending stiffness nearly the same stress and mode at failure as the unreinforced SHS1. It occurred a local introduced buckling of the upper web but without an high impact of the lower CFRP, which didn't fail at all even at high deflections. At SHS4 both, the upper compression and the lower tension web are reinforced mit 2,0mm unidirectional CFRP. This leads to a stable flange elongation without buckling or curving inwards until the upper CFRP fails under compression and the force level drops over a half. The $\pm 45^\circ$ CFRP shear web reinforcement of SHS5 didn't fail at all after application of load but the aluminum compression flange form a plastic buckling pattern (Figure 3 right). The flattening force level reaches a peak which is about 25% below the also flat SHS2 peak load. The four sided CFRP patched SHS6 is similar to the failing behavior of SHS4 with the different of a slight higher maximum force and a load drop which is not as sharp as SHS4. The increased failure load results from the additional reinforcement of the web. Due to the stabilizing edge effect the flange can bear more compressive loading before it fails in a buckling. It can be seen, that the failure of the unidirectional CFRP strap is not caused by reaching its compressive strength but it is initiated by buckling of the upper aluminum flange together with the CFRP strap. Because of the edge stiffness the buckling of the flange leads to a folding of the aluminum web which presses the 45° laminate outwards. (Figure 3 left) This yields to a layerwise cracking of the laminate with a local delamination from the aluminum. SHS7 is reinforced with 2 x 4,0mm unidirectional CFRP. This leads to a similar failure characteristic as SHS4 with 2 x 2,0mm but at a much higher load. After the sudden break of the CFRP, the laminates crack edges slides into each other at ongoing bending deflection while they are delaminating (Fig. 3 middle). This results in an stable decrease of force after the rapid load decrease.

The steel double cap profiles showed similar failure characteristics compared to the square hollow aluminum section profiles, but the steel thickness of 0.7mm leads to instabilities within the area of load introduction. Imperfection in geometry on the basis of joining the two hut profiles in combination with thinner steel webs results in an over all lower failure load. DHP1 failed in plastic folding of the steel flange at half of the SHS1 maximal force. DHP2 and DHP4 failed in the abrupt CFRP compressive instability break with a higher fracture load for 4,0mm reinforcement. Like SHS3, the reinforcements at the tension belt of DHP 3 and DHP 5 didn't fail, they have only an small impact in maximum load. The failure load of the 2.0 mm CFRP reinforcement at DHP6 is at the same level as at DHP2 with its single CFRP application at the top flange.



Figure 3. Typical failure mechanisms. (left) introduced web buckling after compressive instability fiber cracking at flange. (middle) cfrp fiber cracking (SHS7). (right) plastic flange buckling (SHS5)

3.2. Quantitative experimental results

For the aluminum beams the highest fracture load was achieved at the 2x4mm UD-CFRP reinforced SHS7 with $F_{max} = 46.51kN$. The first failure could be noticed at a force level of $R_p = 45.8 kN$.

The all aluminum SHS1 fails due to the local flange buckling at $R_p = 6.8 kN$. Remarkable is the comparison of SHS2 and SHS3 with the same flexural rigidity and structure, but with a different loading direction. The compression reinforced SHS2 fails at a much higher force $R_p = 13.04kN$ compared to $R_p = 7.78kN$ of SHS3. Also the maximum load differs about 68%. With 2mm CFRP upper and lower flange reinforcement the variant SHS4 has a first failure at $R_p = 23.3kN$ and a maximum strength of $F_{max} = 24.3kN$. The $\pm 45^\circ$ shear reinforcement of SHS5 enables a higher R_p of $9.28kN$ than the unidirectional CFRP of SHS3. 4-sided CFRP strips of SHS6 fails at $R_p = 26.19kN$ for the first time and reaches an peak load of $26.5kN$.

Overall the steel double cap profiles fails at a lower force level. This can be justified in the lower wall thicknesses of the metal. This makes the profiles more vulnerable to local deformations at the point of force application. So without CFRP, DHP1 fails at a level of $R_p = 4.2kN$. The upper reinforcement of DHP2 increases the first failure up to $11.42kN$. Same phenomenon can be seen at DHP3 and DHP5 which both, despite strenghtening starts deforming irreversible in the force area of DHP1. There's no benefit of the lower CFRP plate. 4mm CFRP at compressive flange of DHP4 leads to the highest maximum force of $F_{max} = 18.15kN$.

By comparing the elastic energy capacity of the specimens until first failure the values of the aluminum profiles are also higher than for the steel specimen. So 2 x 4mm CFRP increased the bearable elastic energy of SHS7 by the factor 10 compared with unreinforced SHS1 ($388.7 J$ to $38.8 J$). Strengthen the compressive flange is more effective than the tension flange and thicker reinforcement leads to higher maximum forces.

Table 3 shows the quantitive values of the testet specimen.

Table 3. Experimental and theoretical testing results

Specimen	R_p [kN]			F_{max} [kN]	E_{R_p} [J]	$\frac{E_{R_p}}{G}$ [$\frac{J}{kg}$]
	exp.	theor.	Δ [%]	exp.	exp.	exp.
SHS1	6.80	7.20	-5.56	8.45	38.08	30.40
SHS2	13.04	4.4 (13.0)	290 (0.31)	15.69	98.61	68.60
SHS3	7.78	8.80	-11.59	9.35	39.09	27.19
SHS4	23.33	8.2 (26.5)	280 (11.96)	24.32	189.52	116.81
SHS5	9.28	8.50	9.18	12.47	68.52	42.23
SHS6	26.19	9.1 (18.5)	287 (41.57)	26.50	213.60	107.22
SHS7	45.84	12.1(26.5)	403 (72.98)	46.51	388.74	195.15
DHP1	4.20	9.30	-54.84	4.95	28.05	17.12
DHP2	11.42	7.70	48.31	13.47	70.41	38.62
DHP3	4.57	7.70	-40.65	5.89	23.61	12.95
DHP4	12.37	3.70	234.32	18.15	84.19	41.93
DHP5	4.74	3.70	28.11	6.14	21.62	10.77
DHP6	13.25	13.5	-1.85	13.43	84.64	42.15

4. Theoretical results

The analytical investigations, as presented in [5] consider the bending beam as a construct of connected single plates. Each plate is defined as a multilayer composite which stiffnesses are defined by the classical laminate theory. The total stiffness of the beam results from combining all the plates to one whole structure. Boundary conditions and loadings enable the prediction of the beam deformation and so the distortion of each panel. The beam deformation comprise of bending and shear deflection.

This distortions are transformed into the coordinate system of each ply and lead to the stress state in each layer by means of the overall stiffness matrices. Beside a layerwise failure analysis also the local and global stability of the beam (i.e. global beam buckling, lateral torsional buckling, shear buckling of the web and buckling of the flange) is evaluated.

The theoretical results of the first failure force R_p are shown in table 3. Not shown are the well matching theoretical bending stiffnesses compared to the experiment and the beam deflection for first failure. The theoretical values of R_p of certain specimens (SHS2, SHS4, SHS6, SHS7) are split into two parts. The first value gives the theoretical first failure and the brackets fits to the first visible failure mode of the experiments using a linear extrapolation without material degredation. This shows the high potential of a hybrid part designing above the first failure. For the aluminum variants the theoretical and experimental values accord with each other within a deviation of 12%, when the visible failure mode is in focus. Only theoretical predictions of SHS6 (+41,57%) and SHS7 (+72,98%) are conservative. The steel profiles have a much higher uncertainty of R_p between -54,84% (DHP1) and +234,32% (DHP4). As seen in Table 3 the predictions of compressive flange reinforcements remain below the experimentally measured values, while force transmission into metal is overestimatet. This results from local effects, like complex interactions between the metal and composite phase, which can not be represent in analytical calculations so far. R_p symbolized the force of the first failure without mentioning the mode of failure. For each possible mode a failure criterion has to be considered. The theoretical first failure prediction is far below the experimentally detected loads. This is the case for CFRP strengthened compressive flanges in variants SHS2, SHS4, SHS 6 and SHS 7. In Figure 4 the load displacement curve is shown for the aluminum profile SHS4. The displacement represents the displacement of the force application point. Also the theoretical stresses within CFRP and aluminum are plotted. It can be seen, that the yield strength of aluminum ($R_{p0.2} = 140MPa$) is reached at a deflection of 5mm ($S_{theor} = 5.8mm$), while the measured first failure is $R_p = 23.3kN$ at 7.98mm. The stress within the CFRP at break with $\sigma_{CFRP} = 478MPa$ is significantly smaller than its tensile strength from Table 1.

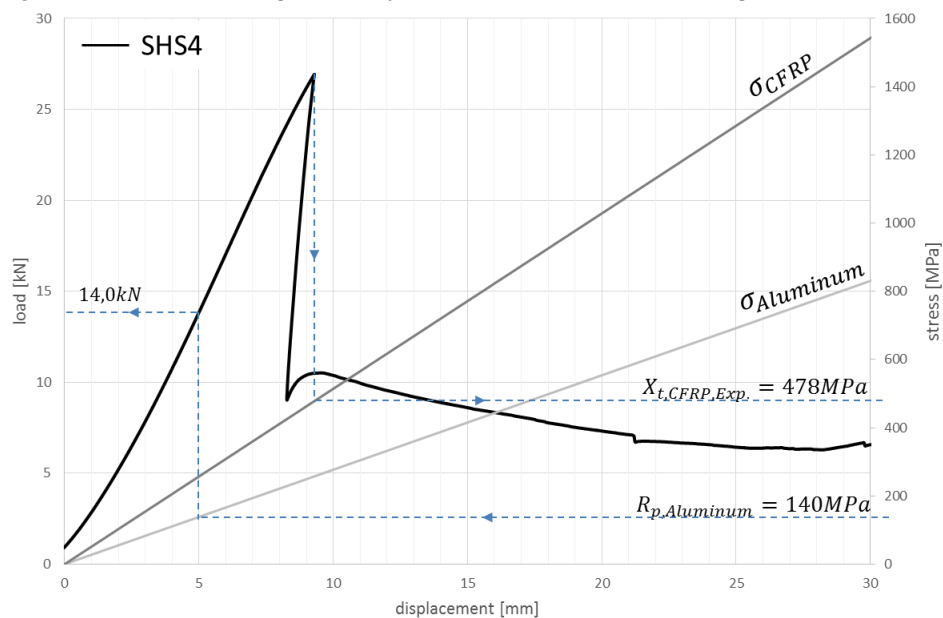


Figure 4. Stress and failure analysis of hybrid bending beam.

5. Conclusions

For a lightweight hybrid part design the principle properties and modes of action for such structures has to be known. For this reason the here described bending tests have been conducted. The results were compared to theoretical predictions in failure load and mode. Some in principle suggestibilities for hybrid part properties have been found. For example increasing the static limit load or elastic energy. Even if it means the forecast has an akzeptable quality for structural design, the local behavior have to be considered. The first failure loading limit is a strong limiting requirement within the automotive industry which dissipates a large potential of hybrid structures and has to be reconsidered.

Acknowledgments

This work was supported by BMW AG. The author wants to thanks the university of applied sciences Munich for the provision of laboratory and the assistance during planning and testing.

- [1] Bambach, M.R., Jama, H.H., Elchalakani, M.: Axial capacity and design of thin-walled steel SHS strengthened with CFRP. *Thin-Walled Structures* 47, pp. 1112-1121, 2009
- [2] Bambach, M.R., Jama, H.H., Elchalakani, M.: Static and dynamic axial crushing of sportwelded thin-walled composite steel-CFRP square tubes. *International Journal of Impact Engineering* 36, pp. 1083-1094, 2009
- [3] Kim, H., Shin, D., Lee, J.: Characteristics of aluminum/CFRP short hollow section beam under transverse quasi-static loading. *Composite: Part B* 51, p. 345-358, 2013
- [4] Jung, D., Kim, H., Choi, N.: Aluminum-GFRP hybrid square tube beam reinforced by a thin composite skin layer. *Composite: Part A* 40, p. 1558-1565, 2008
- [5] Oxenbauer, M., Rother, K.: Methodology for the Design and Optimization of Hybrid Structures in the Early Phase of Vehicle Development. *Proceedings of the American Society for Composites, 30th technical conference, East Lansing, Michigan, USA, Sep. 28-30 2015.*